Appendix for Energy-Aware Coverage Controller Paper

Theorem 2. Using the position controller Eq. (5) and the weight controller Eq. (9) for all robots in a distributed manner, the multi-robot system will asymptotically converge to the stable equilibrium towards the minimum of the locational cost in Eq. (4). i.e.,

$$|p_i - \mathbf{C}_{W_i}| \to 0 \; \forall i \in n.$$

Proof. Let us treat the cost function $H_{\mathcal{W}}$ as a Lyapunov candidate function to demonstrate that the controller drives the multi-robot system to optimal coverage positions. The time derivative of $H_{\mathcal{W}}$ is

$$\dot{H}_{\mathcal{W}} = \sum_{i=1}^{n} \int_{\mathcal{W}_i} (q - p_i)^T \phi(q) dq \dot{p}_i + \sum_{i=1}^{n} \int_{\mathcal{W}_i} \frac{1}{2} \phi(q) dq \dot{w}_i$$

Splitting the above equation into two parts for tractability

$$\dot{H}_{\mathcal{W}} = \dot{H}_1 + \dot{H}_2$$

By applying the position controller $\dot{p}_i$ in Eq. (5),

$$\begin{aligned} \dot{H}_1 &= \sum_{i=1}^{n} \int_{\mathcal{W}_i} (q - p_i)^T \phi(q) dq \, [k_p (C_{\mathcal{W}_i} - p_i)] \\ &= \sum_{i=1}^{n} -k_p M_{\mathcal{W}_i} [(C_{\mathcal{W}_i} - p_i)]^2 \leq 0 \end{aligned}$$

Applying the weight adaptation law in Eq. (9)

$$\dot{H}_2 = -\sum_{i=1}^{n} \frac{1}{2} M_{\mathcal{W}_i} \frac{k_w}{M_{\mathcal{W}_i}} \sum_{j \in \mathcal{N}_i} \left(\frac{w_i}{w_j} - \left(\frac{E_i^{init}}{E_j^{init}} \cdot \frac{\dot{E}_j(t)}{\dot{E}_i(t)} \right) \right)$$

Applying the result of Theorem 1 and Corollary 1, we obtain

$$\dot{H}_2 \approx -\sum_{i=1}^{n} \frac{k_w}{2} \sum_{j \in \mathcal{N}_i} \left(\frac{w_i}{w_j} - \frac{w_i}{w_j} \right) \approx 0.$$

Therefore, $\dot{H}_{\mathcal{W}} \leq 0$, proving the asymptotic convergence of Eq. (12). $\dot{H}_{\mathcal{W}} = 0$ only when the velocity $\dot{p}_i = 0$ for all robots $i \in n$. This can occur only when all the robots reach the centroid of their weighted Voronoi configuration, i.e., the robots converge to their centroids $p_i = C_{\mathcal{W}_i}$, which is the largest invariance set. This concludes the proof.

Alg. 1 provides a summary of the proposed energy-aware controller algorithm distributed in each robot.

Algorithm 1: Energy-Aware Coverage (EAC)

Input: n robots, their positions, and E_{init} (initial energy level or battery capacities).
ϵ, δ : two small positive constants.
Output: Energy-aware weighted region partitions.

while *not converged* **do**
  for *Each robot* r **do**
    Find weighted Voronoi partition W_r (Eq. (3)).
    Find the centroid C_r of W_r.
    Apply the position controller $\dot{p}_r$ given in Eq (5).
    Get information on neighbors' energy and energy depletion rate.
    if $\exists \dot{E}_i(t) - \dot{E}_i(t-1) > 0.2$ **then**
      $E_{init} = E_{current}$
    Apply the energy-aware weight adaptation controller $\dot{w}_r$ from Eq. (9)
    Update w_r and p_r
  if $(\exists E_i(t) < \delta)||(C_i - p_i \leq \epsilon, \forall C_i, p_i)$ **then**
    convergence = True;
    return the energy-aware weighted region partitions.

Additional Experimental Data

Scenario 5 - Non-uniform Density Function

Following [11], we test the proposed energy-aware coverage controller in a non-uniform density environment. A density function ($\phi(q)$ in Eq. (6)) represents the importance of the location, e.g., representing the concentration of events or phenomena in different regions. A high density implies more effort (or time) needed to survey that point of interest, and hence the robots in high-density regions are allocated less area in the coverage. We simulate such a scenario by employing an identical density function as presented in [11], with the following parameter adjustments: $\mu_1 = \begin{bmatrix}2\ 2\end{bmatrix}$, $\mu_2 = \begin{bmatrix}4\ 4\end{bmatrix}$, and $\Sigma = 0.9I$. In this setting, r_1 has higher β ($\beta_1 = 10$) i.e, its $\dot{E}_i(t) = 5$ while all other robots have $\dot{E}_i(t) = 1.4$, however the initial energy and α of all robots remain the same. The results are presented in Fig. 9. Even with a non-uniform density function, the EAC effectively adjusted the weights of robots, resulting in an approximate 50% decrease in cost (-0.31) as compared to WMTC (-0.15) and ATC (-0.16). Furthermore, the EAC demonstrated a remarkable achievement by attaining 140% lower cost than PBC (0.78).

Demonstration in the Robotarium Hardware Testbed

To validate the performance of the proposed controller in the real world, we showcase experiments in two different robot testbeds. The Robotarium's hardware testbed [34] allows us to verify the control accuracy of robots with simulated energy characteristics.

In this demonstration, we used four robots, and robot 2 has a lower initial energy of $E_{init} = 70$ compared to all other robots ($E_{init} = 100$), while their depletion rates are the same. We also simulated a bi-modal density function $\phi(q)$ using the same density

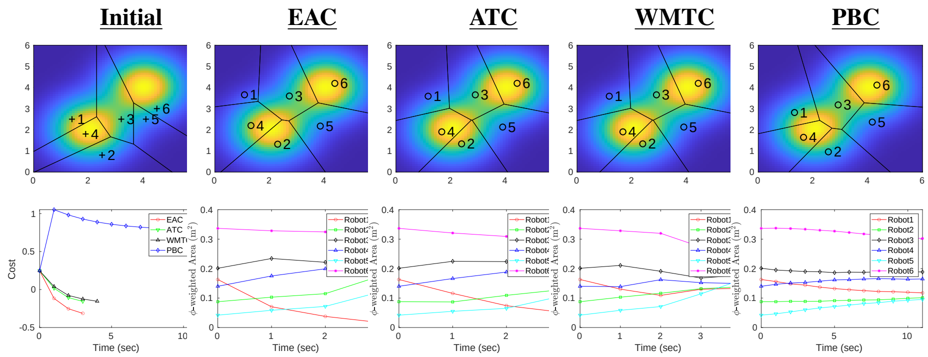

Fig. 9. Results of Scenario 5 experiments (non-uniform density case considering a bi-modal density function). Here, all robots have the same initial energy capacity, but robot 1 has a higher depletion rate). The WMTC coverage treats all robots equally, assigning them based on the region of importance. However, the EAC method correctly assigns robot 1 to a smaller area compared to other methods, due to the depletion rate difference as expected.

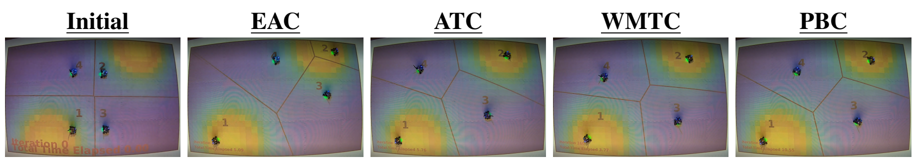

Fig. 10. Real-robot experiment in Robotarium with a bi-modal density function. The robots have similar energy characteristics, but robot 2 (top right) has low initial energy and is close to a source. Both these effects assign significantly less weight (and coverage) to robot 2 in EAC than other controllers.

function mentioned in Scenario 5 (Sec. 13) with two sources closer to robots 1 and 2. We have employed an identical density function as presented in [11], with parameter adjustments: $\mu_1 = \begin{bmatrix}2\ 2\end{bmatrix}$, $\mu_2 = \begin{bmatrix}4\ 4\end{bmatrix}$, and $\Sigma = 0.9I$. We expect the controller to learn the difference between available energy and repartition accordingly. i.e., we expect robot 2 to have a significantly reduced coverage area for two reasons: 1) it has a lower energy capacity, and 2) it is in a region of high importance (high density), which needs to be covered more carefully, further necessitating its weight reduction.

The results for this experiment are presented in Fig 10. Although ATC and PBC assigned a smaller area to robot 2 (primarily due to the influence of the density values), EAC was more effective in allocating a significantly smaller area to it. More results from the simulations and the real-world experiments are included in the attached video. As expected, the bi-modal density function has a source closer to r_2 and this further contributed to the reduction in the weights for r_2 in EAC. Consequently, this increased operational efficiency extends the operational time of r_2, thereby optimizing the overall network lifetime of the robots.

Furthermore, in the main paper, we included the results from experiments conducted on an in-house swarm robotics testbed, which explicates the difference in the coverage control output between a homogeneous and a heterogeneous team of robots where real energy characteristics are considered.